Mimetic Schemes for Hyperbolic Balance Laws

Cory D. Hauck
Continuum Dynamics Group (CCS-2) &
Center for Nonlinear Studies (CNLS)
Los Alamos National Laboratory
cdhauck@lanl.gov

April 4, 2007

1 Introduction

We are interested in constructing mimetic schemes to simulate the behavior of various models of kinetic transport. The models that we consider are typically hyperbolic systems of partial differential equations which express the evolution of a many-particle system as a balance of convective, frictional, and driving forces. In certain asymptotic limits, this balance provides a reduced description of the original model; and in these limits, it is important that a numerical scheme has the same asymptotic properties as the model that it is used to approximate. Mimetic methods are used to create such schemes by enforcing discrete analogs of such asymptotic balances in the discretization procedure.

The mimetic point of view is quite different from the conventional numerical approach to hyperbolic PDE, which emphasizes order of accuracy without much consideration of asymptotic limits. It turns out that for a given mesh spacing h and scaling parameter ε which tends to zero in a particular asymptotic limit, a standard scheme with spatial accuracy of order n will, in fact, be accurate only up to $O(\varepsilon^{-1}h^n)$ terms. Hence for a finite mesh spacing, standard numerical schemes will lose accuracy as $\varepsilon \to 0$. This effect is most noticeable for low order schemes, but may also be observed for higher order schemes near large spatial gradients. In some cases, the loss of accuracy can cause numerical oscillations in a solution; in other cases, numerical solutions with standard schemes will be smooth, but inaccurate.

All of the balance laws we consider can be formulated as an abstract dynamical system of the form

$$\partial_t \mathbf{u} = F(\mathbf{u}, \mathbf{v}) \tag{1a}$$

$$\partial_t \mathbf{v} = G(\mathbf{u}, \mathbf{v}) + \frac{1}{\varepsilon} S(\mathbf{u}, \mathbf{v}) \tag{1b}$$

where the $\mathbf{u}$ and $\mathbf{v}$ are vectored valued functions of space and time. In the limit $\varepsilon \to 0$, $\mathbf{v}$ will relax to a function of $\mathbf{u}$, so that $\mathbf{u}$ completely determines the state of the system in the asymptotic limit. All spatial derivatives and all external and coupled variables have been absorbed into the abstract expressions F, G, and S.

To leading order, asymptotic expansion of $\mathbf{v}$ in powers of ε gives $S(\mathbf{u}, \mathbf{v}) = 0$, which we assume can solved to express $\mathbf{v}$ as a unique function of $\mathbf{u}$:

$$\mathbf{v} = \phi^{(0)}(\mathbf{u}) \,. \tag{2}$$

Thus, to the leading order, $\mathbf{v}$ is given by (2), where $\mathbf{u}$ satisfies

$$\partial_t \mathbf{u} = F(\mathbf{u}, \phi^{(0)}(\mathbf{u})) \,. \tag{3}$$

The first order correction to (2) is

$$\mathbf{v} = \phi^{(0)}(\mathbf{u}) + \varepsilon \phi^{(1)}(\mathbf{u}) \,. \tag{4}$$

where $\mathbf{u}$ now satisfies

$$\begin{aligned} \partial_t \mathbf{u} =& F(\mathbf{u}, \phi^{(0)}(\mathbf{u}) + \varepsilon \phi^{(1)}(\mathbf{u})) \,, \\ =& F(\mathbf{u}, \phi^{(0)}(\mathbf{u})) \\ &+ \varepsilon F_{\mathbf{v}}(\mathbf{u}, \phi^{(0)}(\mathbf{u})) \phi^{(1)}(\mathbf{u}) + O(\varepsilon^2) \,, \end{aligned} \tag{5a}$$

and

$$\begin{aligned} \phi^{(1)}(\mathbf{u}) = & [S_{\mathbf{v}}(\mathbf{u}, \phi(\mathbf{u}))]^{-1} \\ & \left(-\phi^{(0)}_{\mathbf{u}}(\mathbf{u}) \, F(\mathbf{u}, \phi^{(0)}(\mathbf{u})) + G(\mathbf{u}, \phi^{(0)}(\mathbf{u})) \right) . \end{aligned} \tag{6}$$

In analogy with the kinetic theory of dilute gases, the leading order expansion of $\mathbf{v}$ (2) is called the equilibrium or Euler limit and the first order correction (5a) is called the diffusive or Navier-Stokes limit. In this abstract formulation, our goal is to find a consistent, stable discretization for (1) which in the limit $\varepsilon \to 0$ yields consistent, stable discretization for (3) and/or (5a) while maintaining the same order of accuracy.

Our current research is focused on operator splitting techniques for solving (1) in these cases. These techniques address the dynamics of S separately from F and

G. One approach is to break the original system into two component systems:

$$\begin{aligned} \partial_t \mathbf{u} &= 0\,, & \partial_t \mathbf{u} &= F(\mathbf{u},\mathbf{v})\,, \\ \partial_t \mathbf{v} &= \frac{1}{\varepsilon} S(\mathbf{u},\mathbf{v})\,, & \partial_t \mathbf{v} &= G(\mathbf{u},\mathbf{v})\,, \end{aligned} \tag{7}$$

which are then discretized separately. Solving the first component implicitly is the numerical analog of projecting $\mathbf{v}$ onto its equilibrium value, $\phi^{(0)}(\mathbf{u})$. Variations of this splitting have been introduced to ensure that each component is itself a well-posed system [JPT-1998, JPT-2000].

Another approach [JL-1996, NP-2000] is to rewrite (1) in the form

$$\partial_t \mathbf{u} = \lambda F^{(1)}(\mathbf{u},\mathbf{v}) + (1-\lambda) F^{(2)}(\mathbf{u},\mathbf{v})\,, \tag{8a}$$

$$\partial_t \mathbf{v} = \lambda G^{(1)}(\mathbf{u},\mathbf{v}) + (1-\lambda) G^{(2)}(\mathbf{u},\mathbf{v}) + \frac{1}{\varepsilon} S(\mathbf{u},\mathbf{v})\,. \tag{8b}$$

Here the parameter $\lambda \in [0,1]$ is a continuous, monotonic function of ε such that $\lambda|_{\varepsilon \geq 1} = 1$ and $\lambda|_{\varepsilon=0} = 0$. The terms $F^{(1)}$,$F^{(2)}$ and $G^{(1)}$,$G^{(2)}$ are actually exact copies of F and G, respectively; however, they take different discretizations. The discretization of $F^{(1)}$ and $G^{(1)}$ is suited toward the full system (1) while the discretization of $F^{(2)}$ and $G^{(2)}$ is suited to the asymptotic limits equations (3) and (5a). Neither discretization works well for all values of ε; the idea is that a convex combination of them will.

New techniques are now in development which combine the two approaches described above. Roughly speaking, we use the splitting (7) to identify good choices of λ, $F^{(1)}$, $F^{(2)}$, $G^{(1)}$, and $G^{(2)}$ in (8).

2 Diffusive Relaxation

Let us consider examples of diffusive relaxation, when $F(\mathbf{u},\phi(\mathbf{u})) = 0$. In such cases, the diffusive correction $\phi^{(1)}(\mathbf{u})$ is necessary to obtain nontrivial dynamics in the asymptotic limit (see (5a)). Because the of $\phi^{(1)}(\mathbf{u})$ occur over a longer time scale, we let $t \mapsto \varepsilon t$. With respect to this longer time scale, the waves speed of the original hyperbolic system (1) are $O(\varepsilon^{-1})$. For explicit shock-capturing schemes, stability requires a time step of size $O(\varepsilon^{-1}h)$, which is very restrictive for $\varepsilon \ll 1$. Moreover, for problems with shocks or strong discontinuities, implicit schemes are not a sensible alternative.

Below we present several examples, each in non-dimensional form. Thus many physical constants have been absorbed. In all cases, the parameter ε is the ratio of the mean free path of a particle to the characteristic length of the spatial domain. It should be noted due to the longer time scale, the stiff terms in these examples carry an additional factor of ε^{-1} and the diffusive corrections actually appear in the leading order balance.

2.1 Hyperbolic Heat Equation

The simplest example of diffusive relaxation is the linear hyperbolic heat equation in one dimension:

$$\partial_t \rho + \partial_x m = 0\,, \tag{9}$$

$$\partial_t m + \frac{1}{\varepsilon^2}\partial_x \rho = -\frac{1}{\varepsilon^2} m\,. \tag{10}$$

Here ρ is a concentration of particles and m is the bulk momentum of those particles. In the limit $\varepsilon \to 0$, $m = -\partial_x \rho$ and the evolution of ρ is given by the heat equation

$$\partial_t \rho = \partial_x^2 \rho\,. \tag{11}$$

However, when $\varepsilon < h$, standard schemes give numerical results that show excessive numerical dissipation. Operator splitting techniques can be used to improve results in such cases (Figure 1) without sacrificing accuracy in the transport regimes, when ε is no longer small , (Figure 1).

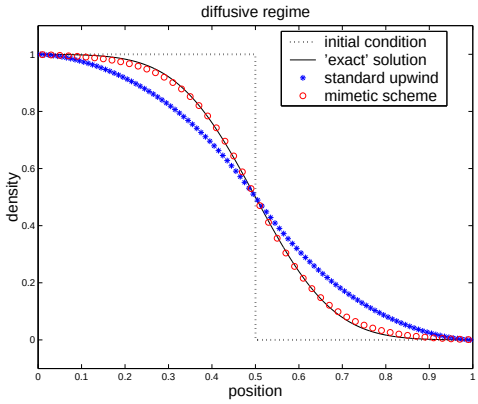

Figure 1: Comparison of standard and mimetic methods for the hyperbolic heat equation in the diffusive regime. 'Exact' solution is computed with 5000 points. Mimetic scheme uses $h = 0.02$ and $\Delta t = 0.004$. Upwind scheme uses $h = 0.01$ and $\Delta t = 4.0 \times 10{-}7$. Both schemes are second order in space and time.

2.2 Radiation Transport

Our motivating application for studying hyperbolic balance laws is radiation transport. In this example photons interact with a static material that absorbs and re-emits photons. In a kinetic theory, these photons are described by a distribution in phase space with coordinates of position x, angle Ω, and frequency ν. When computational resources are limited, this description is often simplified by tracking only a finite number of angular moments of the phase space distribution.

One well-known set of moment equations are the P_n equations. For a slab-symmtric material with monochromatic frequency spectrum, these equations can be

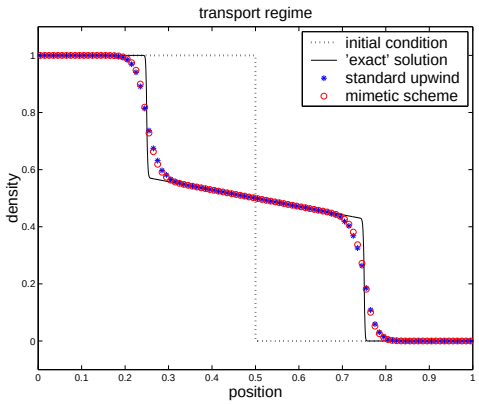

Figure 2: Comparison of standard and mimetic methods for the hyperbolic heat equation in the transport regime. 'Exact' solution is computed with 5000 points. Both schemes use $h = 0.02$ and $\Delta t = 0.004$. Both schemes are second order in space and time.

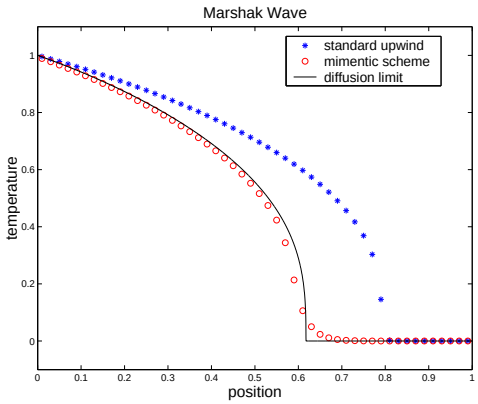

Figure 3: Marshak wave computed with P_7 system in the diffusive regime, $\epsilon = 1.0 \times 10^{-4}$. Mimetic scheme uses $h = 0.02$ and $\Delta t = 0.002$. Upwind scheme uses $h = 0.02$ and $\Delta t = 4.0 \times 10^{-7}$. Both schemes are formally first order in space and time. Solution of (16) is computed using a standard explicit scheme for diffusion with $h = 2.0 \times 10^{-4}$ and $\Delta t = 3.2 \times 10^{-9}$

.

expressed in one spatial dimension in the following non-dimensional form:

$$\partial_t T = -\frac{\sigma}{\varepsilon^2}(\rho_0 - T^4)\,, \tag{12}$$

$$\partial_t \boldsymbol{\rho} + \left(A + \frac{1}{\varepsilon^2}B\right)\partial_x \boldsymbol{\rho} = -\frac{\sigma}{\varepsilon^2}(\boldsymbol{\rho} - \mathbf{r})\,. \tag{13}$$

Here $\boldsymbol{\rho} = (\rho_0, \ldots, \rho_n)^T$ is a vector of angular moments, σ is the scaled cross-section (inverse of mean free path) of the ambient material, T is the material temperature, and $\mathbf{r}$ is a vector whose only non-zero component is $r_0 = T^4$. The matrices A and B are given by

$$A_{ij} = \frac{i+1}{2i+1}\delta_{i,j-1} \quad \text{and} \quad B_{ij} = \frac{i}{2i+1}\delta_{i,j+1}\,, \tag{14}$$

and the matrix $M = A + \varepsilon^{-2}B$ is hyperbolic for all values positive values of ε. In the limit $\varepsilon \to 0$,

$$\rho_i = -\frac{i}{2i+1}\partial_x \rho_{i-1}\,,\ 1 \le i \le n \tag{15}$$

and $\rho_0 = T^4$, where T satisfies

$$\partial_t (T + T^4) = \partial_x \left(\frac{\sigma_0}{3}\partial_x \rho_0\right)\,. \tag{16}$$

For materials with constant cross-section, we have computed solutions of these equations which accurately capture the behavior of (16) in the diffusive limit while circumventing the restrictive hyperbolic time step (Figure 3). These calculations use new techniques with better properties than previous methods. In particular, they allow for a larger time step, avoid black-red discretizations of the diffusive operator, and are able to handle systems with more than two equations. Work continues for more realistic materials with non-constant cross-sections and without slab symmetry.

2.3 Electron Transport

Our final example is a nonlinear hydrodynamic model of a slab symmetric n^+-n-n^+ semiconductor diode. In non-dimensional form, it is given by

$$\partial_t \boldsymbol{\rho} + \partial_x \mathbf{f}(\boldsymbol{\rho}) - \mathbf{l}(\boldsymbol{\rho})\partial_x \Phi = \mathbf{r}(\boldsymbol{\rho}) \tag{17}$$

where

$$\boldsymbol{\rho} = \begin{pmatrix} n \\ nu \\ \frac{nu^2}{2} + \frac{1}{\varepsilon^2}\frac{3n\theta}{2} \end{pmatrix}, \quad \mathbf{l}(\boldsymbol{\rho}) = \begin{pmatrix} 0 \\ \frac{1}{\varepsilon^2}n \\ \frac{1}{\varepsilon^2}nu \end{pmatrix}, \tag{18}$$

$$\mathbf{f}(\boldsymbol{\rho}) = \begin{pmatrix} (nu) \\ nu^2 + \frac{1}{\varepsilon^2}n\theta + \sigma \\ \frac{nu^3}{2} + \frac{1}{\varepsilon^2}\frac{5nu\theta}{2} + \sigma u + \frac{1}{\varepsilon^2}q \end{pmatrix} \tag{19}$$

$$\mathbf{r}(\boldsymbol{\rho}) = \begin{pmatrix} 0 \\ -\frac{1}{\varepsilon^2}\frac{1}{\tau_p}nu \\ -\frac{1}{\varepsilon^2}\frac{1}{\tau_w}\left(\frac{nu^2}{2} + \frac{1}{\varepsilon^2}\frac{3n(\theta-1)}{2}\right) \end{pmatrix} \tag{20}$$

Here n is electron concentration, nu is the current density, θ is the electron temperature density, σ is the viscous stress, q is the heat flux density, and Φ is an electric potential that satisfies a Poisson equation which depends on n. The quantities τ_p and τ_w are (scaled) relaxation times. In the limit $\varepsilon \to 0$, $\theta = 1$ and $u = -\tau_p(\partial_x n - n\partial_x \Phi)$, where n solves the drift-diffusion equation

$$\partial_t n = \partial_x(\tau_p(\partial_x n - n\partial_x \Phi)) \tag{21}$$

and Φ solves the same Poisson equation. Operator splitting techniques based on the balance in (17) that yields (21) improve results even for devices that are *not* operating in the diffusion regime [H-2007]. Such is the case

in Figure 4, where results are computed using a variation of the splitting given in (7). Even though the device behavior is not accurately described by (21), the splitting method can be used to significantly reduce current oscillations at material junctions that are common in standard hyperbolic schemes without degrading accuracy elsewhere.

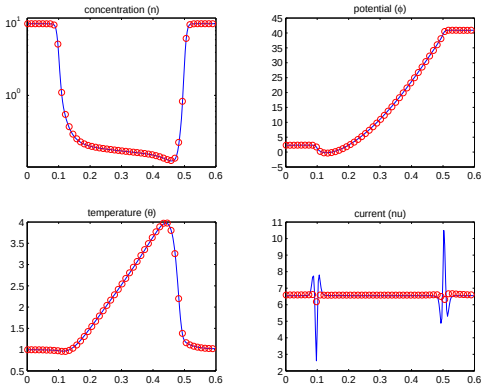

Figure 4: n^+-n-n^+ diode, $\epsilon = 2 \times 10^{-2}$. Both mimetic scheme (red circles) and standard scheme (solid blue) are based on central-upwind discretizations. Both discretizations are second order in space and first order in time. Each scheme uses 200 mesh points and time step is approximately same for both, $\Delta t \sim 1.0 \times 10^{-5}$. The mimetic scheme improves current oscillations in the current profile (bottom right) of the device at material junctions $x = 0.1$ and $x = 0.5$.

References

[H-2007] C. D. Hauck, Numerical Splitting for Hydrodynamic Semiconductor Models, Los Alamos National Labaratory, LAUR 06-8584, *to be submitted to Math. Mod. Meth. Applied Science*.

[JL-1996] S. Jin and C. D. Levermore, Numerical schemes for hyperbolic conservation laws with stiff relaxation terms, J. Comput. Phys., 126 (1996)

[JPT-1998] S.Jin, L.Pareschi, G.Toscani, Diffusive relaxation schemes for multiscale discrete-velocity kinetic equations, SIAM J. Numer. Anal., 35 (1998), pp. 2405-2439.

[JPT-2000] S.Jin, L. Pareschi, G. Toscani, Uniformly accurate diffusive relaxation schemes for multiscale transport equations, SIAM J. Numer. Anal., 38(2000), pp. 913-936.

[NP-2000] G. Naldi and L. Pareschi, Numerical schemes for hyperbolic systems of conservation laws with stiff diffusive relaxation, SIAM J. Numer. Anal., 37, (2000), pp. 1246-1270.